Journal of Manufacturing Innovations
2025, VOL. 1, NO. 3, 08–14
DOI: 10.22055/jomi.2025.48793.1026

New method for fabrication Iron metal foam through powder metallurgy route

Z. Daneshmandi, M.H. Paydar*
Department of Materials Science and Eng., School of Eng., Shiraz University, Shiraz - Iran

ABSTRACT

Iron foam has garnered significant attention across various industries, including automotive, aerospace, medical, and filtration, due to its unique properties. These properties include a high strength-to-weight ratio, excellent energy absorption, and effective sound and thermal insulation. This study evaluates the production of iron foams using the NaCl salt space-holder method. For this purpose, iron oxide powder was used as the raw material, and NaCl salt with a particle size smaller than 180 microns was used as the space-holder. To create a foam with 60% porosity by volume, iron oxide powder was mixed with a specific amount of NaCl space holder of a defined particle size, and the resulting mixture was compacted bidirectionally in a rigid mold under a pressure of 100 megapascals. An initial sintering process was conducted at 800°C for 2 hours. Subsequently, the salt was dissolved in water to extract it from the sample, followed by a final sintering process conducted at 950°C for 2 hours in a pure hydrogen atmosphere to reduce the iron oxide to iron metal. To evaluate the properties of the resulting foam, its microstructure was examined using an electron microscope, and its strength was assessed through compression testing. The results of this study indicated that the produced foam contained approximately 60% porosity with a relatively uniform distribution and was capable of absorbing energy up to approximately 25.35 MJ/m³.

ARTICLE HISTORY
Received 15 January 2024
Revised 27 January 2024
Accepted 27 January 2024

KEYWORDS
Metallic Foam
Iron
NaCl
Powder Metallurgy
Space-holder

1. Introduction

Metal foams, a subset of porous metals, represent a novel class of materials characterized by unique properties such as low density, a high strength-to-weight ratio, a large surface area, excellent sound and thermal insulation, and superior energy absorption [1]. These materials are increasingly utilized across various industrial and research sectors, including medical implants, filters, and shock absorbers. Their most prominent applications are found in the automotive and aerospace industries, due to their exceptional strength-to-weight ratio and outstanding energy absorption capabilities [1-2].

In the medical field, metal foams have gained significant attention in various applications, such as orthopedic implants, scaffolds for tissue repair, and drug delivery systems. The porous structure of metal foam creates a scaffold-like environment that supports bone growth and integration [3]. Its open-cell structure allows bone tissue infiltration, fostering a strong bond between the implant and surrounding bone, which can enhance the long-term stability of orthopedic implants. Mechanically, metal foam can be engineered to possess properties like compressive strength and elasticity that resemble those of natural bone [4]. This mechanical compatibility helps mitigate stress shielding, which occurs when a stiffer implant reduces load transfer to the surrounding bone. By minimizing stress shielding, metal foam implants can potentially reduce the risk of bone resorption and implant loosening. The lightweight nature of metal foam makes it an appealing option for orthopedic implants, particularly in applications such as large joint replacements, where weight reduction is essential. Compared to solid implants, the porous structure of metal foam significantly increases the surface area, which can enhance osseointegration and provide a greater capacity for drug delivery or the attachment of bioactive coatings that promote bone repair and implant integration. Additionally, metal foam can

* Corresponding author.
E-mail address: Paaydar@shirazu.ac.ir (M.H. Paydar)

be easily shaped and machined to meet the specific anatomical needs of patients. This adaptability facilitates the creation of patient-specific implants with complex geometries and appropriate porosity, ensuring better fit, stability, and performance [4-5].

In recent years, extensive studies have been conducted on the fabrication of metal foam [1] from various metals, such as aluminum [6], copper [7], steel [8], titanium superalloys [9], and nickel-titanium shape memory alloys [10]. Generally, metal foams are produced in three states: solid, molten, and vapor. The simplest method involves directly producing foam by injecting gas bubbles into molten metal, enabling the production of large parts at relatively low costs; however, this approach presents the main challenge of irregular and sometimes excessively large pores. Another method uses an open-cell polymer foam as a base mold, similar to investment casting, which is more expensive but results in superior mechanical properties [1, 11]. Solid-state production methods are mainly used for metals with high melting points, with powder metallurgy and the use of gas-releasing agents like TiH2, SrCO3, and MgCO3 being the most prevalent. This approach produces closed-cell foams with acceptable pore distribution and size. Another solid-state method involves space-holder materials, where substances like NaF and NaCl are mixed with metal powder, pressed, and then removed after sintering [11]. This method is particularly applicable to metals with low melting points, like aluminum [1]. Advantages include the ability to control pore size by adjusting the space-holder particle size, approximate uniformity of porosity, ease of processing, and overall controllability of pore size. Due to its relatively simple and low-cost nature, the space-holder method has gained increasing popularity for producing laboratory foam samples. Niu and coworkers [12] produced titanium foam using urea as a space holder, while Hao and et al. [13] produced magnesium foam similarly. Zhao and et al. [10] also produced nickel-titanium alloy foam using NaCl space holder as a space holder. Similar studies have used other materials like NaF and polymers such as PMMA as space holders [1]. The present study explores the production of iron foam using powder metallurgy with NaCl space holder as a space holder and iron oxide as the base material.

2. Materials and Methods

In this study, iron foam was produced using iron oxide Fe_2O_3, with a purity of 98% (industrial purity), and particle size lower than 1 micron, as the iron source and NaCl as space holder. SEM images of the used raw materials are illustrated in Fig. 1. Initially, NaCl space holder with particle sizes smaller than 250 micrometers was prepared using an appropriate sieve. To achieve approximately 60% volumetric porosity, the weight ratio of iron oxide powder, which served as the primary matrix material, to NaCl space holder. was established at 61.84% iron oxide and 38.16% NaCl space holder.

The raw materials were manually mixed in a plastic zip bag with a few drops of ethanol to enhance the mixing process. SEM images for the mixed powders in two different magnifications are shown in Fig. 2. As can be seen, each NaCl particle is well surrounded by Fe_2O_3 particles, creating a homogenous mixture. The resulting powder mixture was then compressed at 150 MPa in a rigid, double-action die (Fig. 3) with a diameter of 10 millimeters for each sample. The compressed samples were pre-baked at a temperature of 800°C for 2 hours. Subsequently, to eliminate the salt, the samples were immersed for three hours in a 500 ml beaker filled with distilled water at 80°C. The water was stirred using a magnetic stirrer to avoid damaging the samples.

The samples were then dried in an oven. At this stage, the mass of the samples was measured, and the mass reduction was calculated. This mass reduction indicated the dissolution of salt in the water. If the changes in mass reduction showed that more than 90% of the salt was removed, the result was considered acceptable, and the subsequent steps were carried out. In the next stage, the samples were placed in a furnace at 950°C for 2 hours to strengthen the bond between Fe_2O_3 particles. After this process, the dimensions and mass of the samples were measured, followed by the reduction process to convert iron oxide to metallic iron in a furnace with a hydrogen atmosphere at 600°C for 1 hour, and then the final baking process at 950°C for 4 hours in the same hydrogen atmosphere. After completing this stage, the mass and dimensions of the samples were measured again, and the degree of reduction was calculated based on the changes (reduction) in

mass. Figure 4 schematically illustrates the stages of foam production.

In this study, the characteristics of the produced foam were analyzed by examining its microstructure with an electron microscope and measuring its compressive strength through a uniaxial compression test.

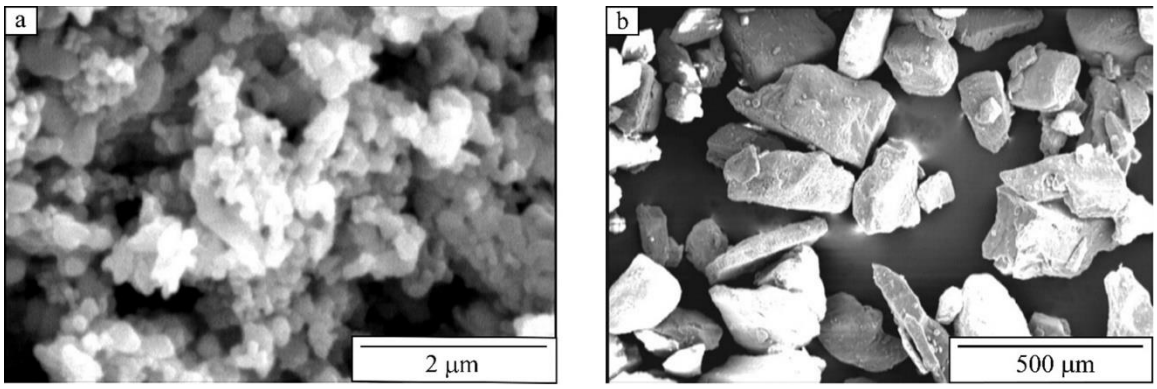


Figure 1. SEM images of a) Fe2O3 and b) NaCl powders used in this study.

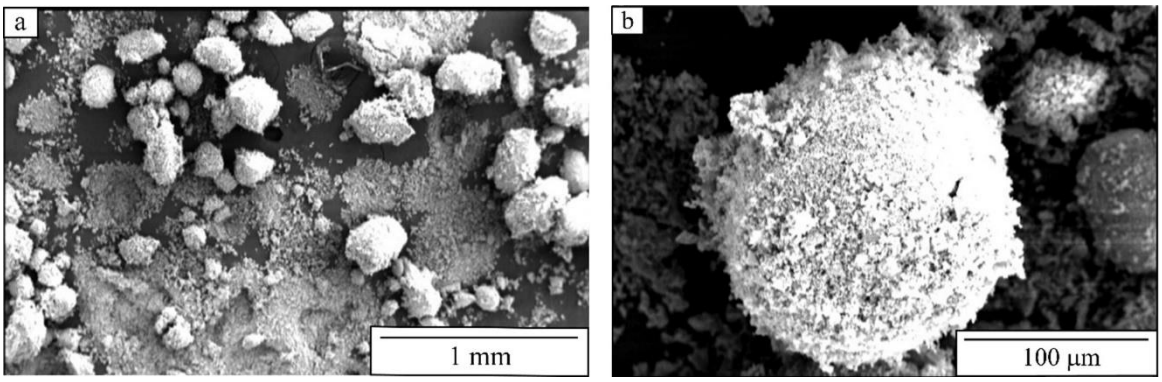


Figure 2. SEM images of Fe2O3-NaCl powders mixture in two different magnifications.



Figure 3. shows the double action die used in the compression process of the iron oxide powder and NaCl space holder mixture.

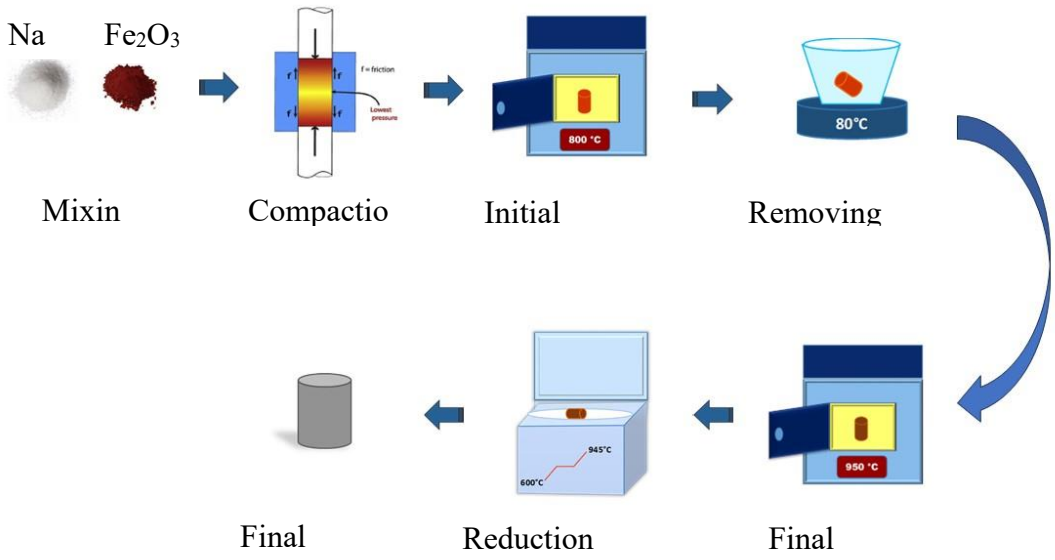


Figure 4. shows a schematic illustration of the process used in producing iron foam by the powder metallurgy method using NaCl space holder as a space holder

3. Results and Discussion

The analysis of the changes in sample weight before and after reduction, as shown in Table 1, indicated that the reduction achieved under the applied conditions exceeded 90 percent. Additionally, the resulting metal foam displayed a metallic sheen. The residual porosity in the sample after the sintering process, based on the data presented in Table 1, was calculated to be approximately 60 percent by volume, which aligns with the initial design specifications.

Table 1. details the specifications of the sample (mass and dimensions) before and after the reduction process.

Parameters / Sample	m_0 (g)	m_1 (g)	d_0 (mm)	d_1 (mm)	H_0 (mm)	H_1 (mm)	% Reduction
1	2.4598	2.0035	10.11	10.05	11.98	11.78	90.1

Figure 5 presents an electron microscope image of the outer surface of the foam produced at two different magnifications. These images reveal a relatively uniform distribution of pores, which exhibit a somewhat irregular and angular shape that corresponds to the salt particles used as space holders. A closer examination of the image at higher magnification clearly indicates that the connections between the reduced iron oxide particles are well established, and the structure demonstrates good coherence in the walls. However, a small number of very tiny pores, in comparison to the main pores of the foam, remain within the walls.

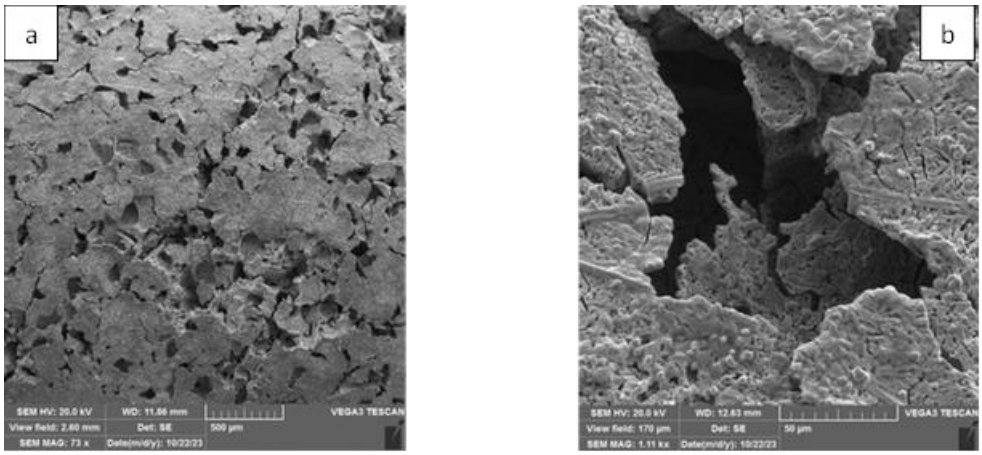


Figure 5. a) View of the wall (external surface) of the produced foam, b) Close-up view of the same wall.

The results of the pressure test conducted on the produced foam sample are presented in Figure 6. This figure illustrates the deformation behavior of the foam during the pressure test, which can be categorized into three distinct regions: the elastic region, the plateau region, and the densification region. The results indicate that plastic deformation begins at a stress of approximately 20 MPa. Additionally, the average stress in the plateau region—where the foam experiences its maximum strain is around 35 MPa. The compression behavior and mechanical strength of the iron foam fabricated in this study are somewhat similar to the mechanical properties of the stainless-steel foam fabricated through the powder metallurgy route, where carbamide was used as a space holder and randomly mixed with stainless steel powder to create a foam with approximately 65% porosity [14]. However, it should be note that, the mechanical properties of metal foams critically depend on the base materials, volume percentage of the remaining porosities, size and distribution of the porosities and density of the cell walls [15]. To determine the foam's energy absorption capability, the area under the stress-strain curve in the plateau region (up to a maximum strain of about 0.65) was calculated according to Equation (1) and plotted as a function of strain (Figure 7). Additionally, the energy absorption efficiency (E) was calculated using Equation (2) and plotted as a function of strain (Figure 8).

$$w = \int_0^{\varepsilon} \sigma d\varepsilon \qquad (1)$$

$$E = \frac{\int_0^{\varepsilon} \sigma d\varepsilon}{\sigma} \qquad (2)$$

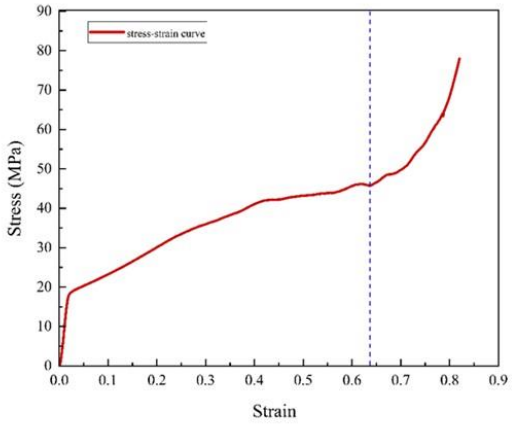


Figure 6. shows the stress-strain curve of the foam produced with 60% volumetric porosity in a uniaxial compressive test.

As illustrated in Figure 7, the maximum energy that can be absorbed by the produced foam is approximately 25 MJ/m³. Given the stability of the plateau region up to a strain of 0.65 and the condition of the foam after the compression test, it can be concluded that the produced foam possesses desirable plastic deformation capabilities and effectively absorbs energy due to its porosity and the appropriate ductility of the walls within the foam structure.

Figure 8 illustrates the energy absorption efficiency of foam with a volume porosity of 60%. Energy absorption efficiency is a metric that quantifies the amount of energy a material absorbs (up to a specific strain) relative to the maximum energy absorbed before failure. The energy absorption efficiency curve is divided into three distinct regions: (1) the steep increase region,

where the energy absorption efficiency rises sharply with increasing strain until it reaches a peak;

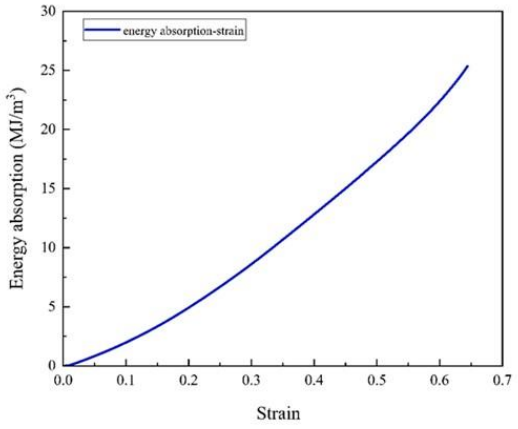


Figure 7. shows the energy absorbed as a function of the strain of the produced foam sample.

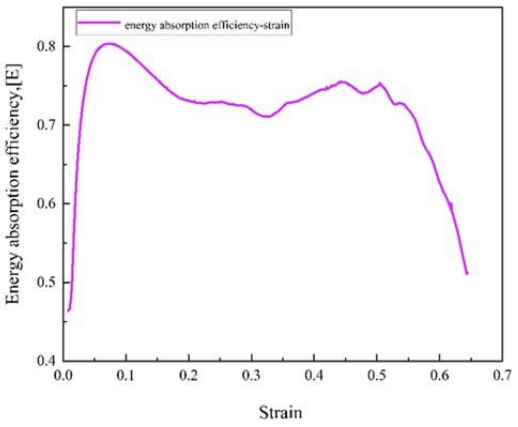


Figure 8. shows the energy absorption efficiency vs the strain of the produced foam sample.

(2) the stability region, where the efficiency experiences a slight decrease and stabilizes at a certain level, although it may occasionally exhibit fluctuations, indicating foam instability during the compression process; and (3) the weakening region, where the energy absorption efficiency declines sharply as strain increases. As seen in Figure 8, the energy absorption efficiency for our produced sample reaches a maximum in the range of 70% to 80%, with this maximum efficiency occurring at strains between 0.1 and 0.5.

4. Conclusions

This research introduces a novel method for the effective production of iron foam, utilizing iron oxide as the raw material and NaCl as a space holder. The resulting foam exhibits a volume porosity of 60%. Compression testing revealed that the yield strength of the foam is approximately 20 megapascals, with a plateau region extending to a strain of about 0.65. Furthermore, the energy absorption capacity of the foam is approximately 25 MJ/m³ at a strain of 0.65, and the energy absorption efficiency within the strain range of 0.1 to 0.5 was found to be relatively stable, fluctuating between 70% to 80%.

References

[1] M.F. Ashby, Metal foams: a design guide, Butterworth-Heinemann, Boston, 2000.

[2] F. Hassanli, M.H. Paydar, Improvement in energy absorption properties of aluminum foams by designing pore-density distribution, Journal of Materials Research and Technology 14 (2021) 609–619. https://doi.org/10.1016/j.jmrt.2021.06.073.

[3] J. Banhart, Manufacture, characterisation and application of cellular metals and metal foams, Progress in Materials Science 46 (2001) 559–632. https://doi.org/10.1016/S0079-6425(00)00002-5.

[4] K. Alvarez, H. Nakajima, Metallic Scaffolds for Bone Regeneration, Materials 2 (2009) 790–832. https://doi.org/10.3390/ma2030790.

[5] F. Matassi, A. Botti, L. Sirleo, C. Carulli, M. Innocenti, Porous metal for orthopedics implants, Clin Cases Miner Bone Metab 10 (2013) 111–115.

[6] R. Surace, L.A.C. De Filippis, E. Niini, A.D. Ludovico, J. Orkas, Morphological Investigation of Foamed Aluminum Parts Produced by Melt Gas Injection, Advances in Materials Science and Engineering 2009 (2009) 506024. https://doi.org/10.1155/2009/506024.

[7] Q.Z. Wang, C.X. Cui, S.J. Liu, L.C. Zhao, Open-celled porous Cu prepared by replication of NaCl space-holders, Materials Science and Engineering: A 527 (2010) 1275–1278. https://doi.org/10.1016/j.msea.2009.10.062.

[8] C.Y. Zhao, T.J. Lu, H.P. Hodson, J.D. Jackson, The temperature dependence of effective thermal conductivity of open-celled steel alloy foams, Materials Science and Engineering: A 367 (2004) 123–131. https://doi.org/10.1016/j.msea.2003.10.241.

[9] S. Ahmad, N. Muhamad, A. Muchtar, J. Sahari, K.R. Jamaludin, M.H.I. Ibrahim, N.H. Mohamad Nor, I. Murtadhahadi, Producing of titanium foam using titanium

alloy (Al3Ti) by slurry method, in: International Conference in Engineering and Technology, 2008.

[10] X. Zhao, H. Sun, L. Lan, J. Huang, H. Zhang, Y. Wang, Pore structures of high-porosity NiTi alloys made from elemental powders with NaCl temporary space-holders, Materials Letters 63 (2009) 2402–2404. https://doi.org/10.1016/j.matlet.2009.07.069.

[11] N. Babcsán, J. Banhart, D. Leitlmeier, Metal foams-manufacture and physics of foaming, in: The International Conference Advanced Metallic Material, 2003.

[12] W. Niu, C. Bai, G. Qiu, Q. Wang, L. Wen, D. Chen, L. Dong, Preparation and characterization of porous titanium using space-holder technique, Rare Metals 28 (2009) 338–342. https://doi.org/10.1007/s12598-009-0066-7.

[13] G.L. Hao, F.S. Han, W.D. Li, Processing and mechanical properties of magnesium foams, J Porous Mater 16 (2009) 251–256. https://doi.org/10.1007/s10934-008-9194-y.

[14] M. Mirzaei, M.H. Paydar, A novel process for manufacturing porous 316 L stainless steel with uniform pore distribution, Materials & Design 121 (2017) 442–449. https://doi.org/10.1016/j.matdes.2017.02.069.

[15] M.F. Ashby, R.F.M. Medalist, The mechanical properties of cellular solids, Metall Trans A 14 (1983) 1755–1769. https://doi.org/10.1007/BF02645546.